Amino acid immobilization of copper surface diffusion on Cu(111)

Nathan P. Guisinger[1], Andrew J. Mannix[1,2], Rees B. Rankin[4], Brian Kiraly[1,2], Jesse A. Phillips[5], Seth B. Darling[1], Brandon L. Fisher[1], Mark C. Hersam[2,3], Erin V. Iski[5†]

[1]Center for Nanoscale Materials, Argonne National Laboratory, 9700 South Cass Avenue, Building 440, Argonne, IL 60439, USA

[2]Department of Materials Science and Engineering, Northwestern University, 2220 Campus Drive, Evanston, IL 60208, USA

[3]Department of Chemistry, Northwestern University, 2220 Campus Drive, Evanston, IL 60208, USA

[4]Department of Chemical Engineering, Villanova University, 800 E Lancaster Ave, Villanova PA 19085, USA

[5]Department of Chemistry and Biochemistry, University of Tulsa, 800 South Tucker Drive, Tulsa, OK 74104, USA

[†]Corresponding Author: erin-iski@utulsa.edu

Abstract

Surface diffusion and molecular self-assembly are two critically important processes in chemistry and nature. We report that amino acids deposited on a Cu(111) surface drive a separation at the two-dimensional limit between self-assembling molecules and diffusing copper atoms. Since the self-assembling amino acids prefer non-planar, tridentate bonding with neighboring adatoms, they attach to and immobilize diffusing copper adatoms on the surface. This chemical interaction freezes out the copper diffusion causing the condensation of “solid” copper adatom islands on the surface. We observe such a separation and immobilization for eight different amino acids, suggesting the generality of this phenomenon beyond a single amino acid species. Furthermore, at elevated temperatures, a disruption of the prototypical Ostwald ripening of adatom islands is also observed. These results provide fundamental insight into chiral molecular self-assembly and its interplay with metal atom surface diffusion.

Surface diffusion is a fundamental physical process that involves the movement of atoms or molecules in two-dimensions (2D)[1-4]. It is a critical component of surface science and is at the heart of numerous technologies ranging from material synthesis and thin film growth to catalysis and energy storage[5-11]. In chemistry, molecular self-assembly relies on surface diffusion and subsequent molecule-molecule interactions and is utilized as a powerful strategy to enhance numerous technological platforms[12-16]. It also serves as a foundational element of modern nanotechnology through its "bottom-up" approach towards fabrication at the nanoscale. These strategies are omnipresent in nature where the self-assembly of organic molecules underlies most biological processes. For example, amino acids are known to form chiral supramolecular assemblies on various substrates with intricate long-range ordering[17-19]. The study of amino acid self-assembly can thus enhance our understanding of fundamental biological processes, such as chiral selectivity and recognition[20, 21].

In our ongoing efforts to explore the surface chemistry of amino acids on Cu(111)[22, 23], we observe behavior that is absent from conventional molecular self-assembly. To date, all of the amino acids that we have investigated at intermediate surface coverages (30% - 70% of a monolayer) self-assemble into their own distinct molecular superstructures. However, even though each amino acid exhibits unique molecular ordering based on its associated molecular backbone, we have observed a shared, common property where they *all* disrupt and immobilize the diffusion of Cu atoms on the underlying surface. The result of this immobilization is the formation of isolated Cu islands of distinct sizes and

shapes that are dispersed across the surface and throughout the capping molecular superstructures.

The deposition of amino acids is performed with the Cu(111) substrate at room temperature (RT), where it is known that the surface is a 2D gas of diffusing Cu atoms[24-26]. These studies were performed in an ultrahigh vacuum (UHV) environment at the atomic-scale utilizing scanning tunneling microscopy (STM). The conditions of the amino acid dose (both the deposition rate and surface coverage) strongly influences the resulting Cu adatom immobilization and island formation. For higher dosing rates and larger molecular coverages, the surface is quickly saturated with amino acid molecules; the resulting Cu islands are observed with greater frequency and size variation. We are defining saturated coverage as molecular packing that does not expose the underlying Cu substrate and low-coverage as containing regions of exposed substrate. At lower dosing rates (resulting in lower coverages), molecular self-assembly into various superstructures is more prevalent, and while copper islands still exist, they are most pronounced for amino acids of higher molecular weight and a corresponding increased molecular “footprint”. In addition, the amino acid immobilization of Cu atoms allows for the observation of several fundamental elements of surface diffusion that are inherent to a more “natural state” of the Cu(111) surface. Traditionally, fundamental studies of surface diffusion on metal surfaces require the deposition of metal adatoms onto the surface[27-29], which is not necessary for this system. Finally, when scanned at elevated temperatures to observe diffusion dynamics and stability of the Cu islands, we found that the amino acids disrupted

the expected Ostwald ripening of the islands and that all islands diminish in size over time[30, 31]. This 2D separation between amino acid molecules and diffusing Cu adatoms not only provides a unique example of molecular self-assembly, but also reveals a platform to investigate the fundamental mechanisms of heterogeneous surface diffusion.

Results and Discussion

The amino acids are deposited onto the Cu(111) surface at room temperature followed by a 10 - 15 min anneal at ~ 450 K to drive self-assembly, significantly below the decomposition temperature of the amino acids[32]. The samples are then cooled to 55 K and imaged at the atomic-scale with the STM. When an amino acid initially adsorbs on a metal surface, it is energetically favorable for the molecule to deprotonate and form a tridentate bond[33-38], where the two oxygen atoms in the carboxylic group and the nitrogen in the amine group attach to the surface, as schematically illustrated in Fig. 1(a). This is a universal bonding motif for the amino acids on Cu(111) and results in a tripod structure with the functional “R” group angled off of the surface (which can depend on chirality). Since the deposition is at room temperature along with a subsequent thermal anneal, the amino acids will diffuse on the surface and self-assemble via hydrogen bonding and van der Waals attractions. The main components of the molecular self-assembly are the tridentate interaction with the Cu(111), thermal annealing to enhance surface diffusion of the molecules, and finally hydrogen bonding between the amino acids that locks them into a self-assembled structure. At the same time,

both at room temperature and during the annealing step, copper atoms are diffusing over the surface, as illustrated in Fig. 1(b). Based on these observations, we hypothesize that the diffusing molecules interact with the diffusing copper atoms in a manner in which the amino acids are switching from a planar tridentate bonding motif to a tilted tridentate motif with a neighboring Cu atom. Due to decreased coordination, the amino acid molecules preferentially interact with and immobilize a diffusing Cu atom, as illustrated in the insets of Fig. 1(b). Figure 1(b) further illustrates that when the coverage of amino acids increases, the immobilization of diffusing atoms results in the formation of encapsulated Cu islands.

It is important to note, experimentally, that the first amino acid structures to form, even at the lowest coverages, are located along the step-edges and are typically one molecule thick (Supplementary Fig. 1). Step-edges are a preferential site of molecular attachment due to decreased coordination of the metal atoms at those sites. In addition, because the amino acids robustly and preferentially passivate the step-edges with tilted tridentate bonds, it appears that those bonds are more stable (stronger) than the tridentate interaction forming on the flat terrace. This observation supports preferential binding to a neighboring (or nearby diffusing) Cu atom. In addition, the source and sink of the diffusing Cu atoms on a clean surface are from the step-edges. If these step-edges are passivated with amino acids, they will impede diffusing Cu atoms from leaving and returning to the step-edge and ultimately enhance the formation of metal islands.

In this study, we explored 8 different, essential and non-essential amino acids (L-chirality throughout) that are listed by increasing molecular weight as follows: alanine, serine, threonine, cysteine, isoleucine, histidine, phenylalanine, and tryptophan. These molecules represent a sampling of different amino acid molecular structures with polar and nonpolar side chains. The immobilization is illustrated in the STM image of Fig. 1(c), which shows the formation of numerous Cu islands following the deposition and self-assembly of isoleucine. The coverage of isoleucine molecules is about 40% of a complete monolayer. The STM image of Fig. 1(d) zooms in on the isoleucine molecular assembly which is comprised of random, chain-like structures. In this case, we can see three Cu islands that have tightly packed amino acids around their entire circumference and random isoleucine chains forming on top of the islands, consistent with the surrounding assemblies on the flat Cu(111) terrace.

We find that the molecular coverage needed to observe the immobilization of diffusing surface atoms and the formation of the islands depends on the molecular weight of the amino acid, in some ways analogous to the molecular “footprint”. For the lower molecular weight amino acids (alanine (89.09 g/mol), threonine (119.12 g/mol), and cysteine (121.16 g/mol)), immobilization and Cu island formation is observed near a full monolayer, while isoleucine (131.17 g/mol), histidine (155.15 g/mol) and tryptophan (204.23 g/mol) exhibit immobilization at a lower coverage (Supplementary Fig. 2). For all of the amino acids studied, the immobilization is most pronounced near a complete monolayer coverage. At first glance, the Cu islands observed at a full monolayer appear to be the formation of

a second molecular layer. However, at a lower surface coverage of the higher molecular weight amino acids, such as tryptophan, we clearly see that the self-assembly was immobilizing Cu diffusion that resulted in the formation of copper islands, as illustrated in Fig. 2(a). As expected, tryptophan self-assembles differently than isoleucine and forms well-ordered molecular chains that are two molecules wide. Again, there is tight molecular ordering surrounding the islands and the step-edges. To further verify that these are indeed copper islands, we utilized scanning tunneling spectroscopy (STS) to plot a 2D conductance map that spatially plots the local density of states (LDOS). The 2D conductance map in Fig. 2(c) was taken concurrently with the zoomed in topographic image of Fig. 2(b). We can see for the island outlined by the dashed box that the bare areas of the island have the same contrast/LDOS as the bare copper on the surrounding terrace, whereas the LDOS of the molecules is clearly different. Furthermore, we measured a cross-section of an immobilized island of copper atoms, Fig. 2(d), and can clearly see that the islands are the height of a single Cu(111) step.

Figure 3 illustrates the immobilization of diffusing Cu atoms for eight of the amino acids that we investigated (a, alanine; b, serine; c, cysteine; d, threonine; e, isoluceine; f, histidine; g, phenylalanine; and h, tryptophan). At low surface coverage, each of these amino acids exhibits a unique molecular self-assembly. However, the immobilization of diffusing Cu atoms appears to be a universal characteristic for all of these amino acids. Past a certain low threshold coverage, each amino acid will immobilize copper surface diffusion resulting in a separation between the self-assembling molecules and the diffusing copper atoms. Past work

indicates that there are metal-organic molecular assemblies that utilize diffusing atoms on the surface in order to form molecular networks[39-41]. Metal-organic frameworks cannot be fully ruled out in all amino acid self-assembly, but it is not apparent in any of our low coverage molecular networks. This also brings forward a concern that perhaps we are observing molecular etching of the copper surface, where the islands are remnants of the previous terrace. There are two observations that preclude this interpretation: (1) Etching that results in the production of adatom islands also produce vacancy islands, which are rarely observed and only for cysteine (due to the presence of sulfur). (2) The Cu island density scales with molecular coverage, which is expected, but we do not observe a higher etching rate for a higher molecular coverage. In other words, we would expect more aggressive etching at a full monolayer coverage, but the terraces below the islands are always intact and support molecular assembly. We do observe ordered modification of the step-edges for some of the amino acids[42-44] (Supplementary Fig. 3).

In order to study the dependence of island formation on temperature and annealing, we studied a surface right after the deposition of isoleucine (no annealing) followed by a 15 min. and 90 min. anneal at 450 K, as illustrated in Fig. 4. Importantly, as before, the surface was at room temperature during deposition and that the images were taken at 55 K. Immediately after deposition without an anneal, we see that the amino acids have immobilized the Cu atoms and they appear as small clusters within the network (Fig. 4(a)). It is quite interesting to observe that even though the Cu adatoms are immobilized within the amino acid

network, given enough thermal energy they will diffuse within that network. Following our standard 15 min. anneal at 450 K to drive self-assembly, the small clusters of trapped Cu adatoms coalesce within the amino acid network to form islands, as illustrated in Fig. 4 (b). Annealing longer than 90 min., Fig. 4 (c), results in the formation of larger islands across the surface. It is at this point that we begin to observe a breakdown of Ostwald ripening that is expected for a bare Cu surface.

It has been previously established that adatom diffusion on a clean copper surface follows an Ostwald ripening mechanism[31, 45], whereby smaller islands decay and shrink, while larger islands grow in size. This is facilitated by a mass transfer through adatom diffusion from smaller islands to larger, more thermodynamically stable islands. These studies require the evaporation of adatoms onto a clean surface in order to generate metal islands followed by the characterization of island decay. The Ostwald ripening of copper islands can easily be observed with STM at room temperature on pristine surfaces[31, 45, 46]. In this study, however, copper adatom diffusion is tracked within the context of the heterogeneous two-species system. We observe islands surrounded and immobilized by a self-assembled molecular layer. As such, we observe no decay or ripening of our islands at room temperature. In order to enhance diffusion, we characterized these surfaces at an elevated temperature (350 K), as illustrated in Fig. 5. In Fig. 5(a), we show a series of images taken over a 44 hour time period for a full monolayer of cysteine molecules at an elevated temperature. Over time, we observe the decay of all islands (both adatom and vacancy islands) with no apparent Ostwald ripening. This result is also confirmed with Cu islands among a

monolayer of isoleucine molecules, illustrated in the image series of Fig. 5(b), which exhibit decay from t1 (1 hr) to the final time of t4 (24 hr). Fig. 5(c) shows the analysis of island decay for the cysteine sample illustrated in Fig. 5(a). The plot clearly shows two regimes of island decay characterized by differing decay rates. The first is relevant for a critical island area of 100 nm^2 or below, where the islands completely disappear at a relatively rapid pace. While the second regime characterizes the slower decay of larger islands (>100 nm^2). These initial results demonstrate the potential for further surface science studies focused on the interplay of Cu diffusion in the presence of a molecular layer and the special stability associated with islands of a certain size.

In conclusion, we have investigated a unique separation between self-assembling amino acids and diffusing Cu adatoms on a Cu(111) surface. This separation is mediated by preferentially tilted, tridentate bonding between the amino acids and diffusing Cu atoms, which slows down and immobilizes the diffusion of the Cu. This immobilization has been observed for 8 different amino acids and appears to be a general property, distinct from molecular self-assembly. The observed separation shows a dependence on the dose rate, surface coverage, and the molecular weight of the amino acid. Increased molecular dosing rates and higher molecular coverages lead to an increase in Cu island density within the molecular network. Higher molecular weight amino acids exhibit immobilization at lower coverages due to an increased interaction with the surface. The immobilization results in a disruption of Ostwald ripening that is otherwise expected for the Cu(111) surface. It is worth noting that the amino acids are chiral

molecules and this immobilization may have relevance in the study and encapsulation of adatoms on high index chiral metal surfaces[47-49]. Overall, this molecular encapsulation of diffusing metal adatoms presents a unique platform for studying heterogeneous diffusion processes in the 2D limit.

METHODS

Experiments were performed in an ultrahigh-vacuum scanning tunneling microscope (UHV-STM, Omicron Technology). The STM was cooled using liquid helium to a temperature near 55 K. The Cu(111) sample was cleaned using repeated cycles of Ar^+ sputtering and annealing at 900 K. The cleanliness of the sample was verified using STM imaging. The amino acid molecules were purchased from Sigma-Aldrich. The molecules were loaded into a 4-cell molecular doser that was separated from the preparation chamber with a gate valve. The doser was equipped to heat at constant temperatures using a water-cooled line for stability. The amino acid molecules were adsorbed under UHV conditions onto a clean Cu(111) surface at room temperature. The temperatures used to sublimate the amino acids for dosing were well below the decomposition temperature of the molecules (i.e. heated isoleucine to ~ 450 K). Unless otherwise indicated, after molecular dosing the surfaces were annealed in the STM chamber to 450 K for 15 minutes to drive self-assembly. All of the images were taken with the sample cooled to 55 K with liquid helium. STM images were obtained with chemically etched W tips at bias voltages between -2 to +2 V and tunneling currents between 50 and 100 pA. Once the tips were moved into the STM chamber, they received e-beam bombardment to remove oxidation and to increase sharpness. Differential conductance (dI/dV) images were acquired using a lock-in amplifier. For the images used to watch the dynamics of the islands, the surface was held at 350 K while the tip scanned for 44 hours. Drift was corrected using landmarks of the surface to ensure that the same area was examined.

DFT calculations were performed with the VASP code as a standalone package and as implemented through the MedeA environment[50-53]. Calculations used the PAW-GGA functional[54-56], 0.2 eV Methfessel-Paxon fermi smearing[57], and a 2x2x1 k-point grid in reciprocal space. Electronic structure minimization was converged to at least 10^-6 eV per calculation, and force minimization were converged to less than 0.04 eV for relaxed atoms. Calculations were performed with a 19 atom Cu adatom island at approximately a 1/14th ML coverage with symmetric registry to an ideal Cu(111) surface. The calculation slab was 4 layers thick (excluding Cu adatom island), and had 25 of spacing in the direction parallel to the surface normal. Isoleucine was used as the probe adsorbate molecule, and its coverage was varied up to 6 molecules per 19atom ad-island.

REFERENCES

1. G Ehrlich, a.; Stolt, K., *Annu. Rev. Phys. Chem.* **1980,** *31* (1), 603-637.
2. Naumovets, A. G.; Vedula, Y. S., *Surf. Sci. Rep.* **1985,** *4* (7), 365-434.
3. Jaklevic, R. C.; Elie, L., *Phys. Rev. Lett.* **1988,** *60* (2), 120-123.
4. Mo, Y. W.; Kleiner, J.; Webb, M. B.; Lagally, M. G., *Phys. Rev. Lett.* **1991,** *66* (15), 1998-2001.
5. Zhang, Z.; Lagally, M. G., *Science* **1997,** *276* (5311), 377-383.
6. Venables, J. A.; Spiller, G. D. T.; Hanbucken, M., *Rep. Prog. Phys.* **1984,** *47* (4), 399.
7. Kapoor, A.; Yang, R. T.; Wong, C., *Cat. Rev.* **1989,** *31* (1-2), 129-214.
8. Rolison, D. R., *Science* **2003,** *299* (5613), 1698-1701.
9. Liu, C.; Li, F.; Ma, L.-P.; Cheng, H.-M., *Adv. Mater.* **2010,** *22* (8), E28-E62.
10. Dillon, A. C.; Jones, K. M.; Bekkedahl, T. A.; Kiang, C. H.; Bethune, D. S.; Heben, M. J., *Nature* **1997,** *386*, 377.
11. Xie, Y.; Naguib, M.; Mochalin, V. N.; Barsoum, M. W.; Gogotsi, Y.; Yu, X.; Nam, K.-W.; Yang, X.-Q.; Kolesnikov, A. I.; Kent, P. R. C., *J. Am. Chem. Soc.* **2014,** *136* (17), 6385-6394.
12. Barth, J. V.; Costantini, G.; Kern, K., *Nature* **2005,** *437*, 671.
13. Lopes, W. A.; Jaeger, H. M., *Nature* **2001,** *414*, 735.
14. Love, J. C.; Estroff, L. A.; Kriebel, J. K.; Nuzzo, R. G.; Whitesides, G. M., *Chem. Rev.* **2005,** *105* (4), 1103-1170.
15. Bartels, L., *Nat. Chem.* **2010,** *2*, 87.
16. Hla, S.-W.; Bartels, L.; Meyer, G.; Rieder, K.-H., *Phys. Rev. Lett.* **2000,** *85* (13), 2777-2780.
17. Humblot, V.; Barlow, S. M.; Raval, R., *Prog. Surf. Sci.* **2004,** *76* (1), 1-19.
18. Barlow, S. M.; Raval, R., *Curr. Opin. Colloid Interface Sci.* **2008,** *13* (1), 65-73.
19. Costa, D.; Pradier, C.-M.; Tielens, F.; Savio, L., *Surf. Sci. Rep.* **2015,** *70* (4), 449-553.
20. Chen, Q.; Richardson, N. V., *Nat. Mater.* **2003,** *2*, 324.
21. Kühnle, A.; Linderoth, T. R.; Hammer, B.; Besenbacher, F., *Nature* **2002,** *415*, 891.
22. Yitamben, E. N.; Niebergall, L.; Rankin, R. B.; Iski, E. V.; Rosenberg, R. A.; Greeley, J. P.; Stepanyuk, V. S.; Guisinger, N. P., *J. Phys. Chem. C* **2013,** *117* (22), 11757-11763.
23. Yitamben, E. N.; Clayborne, A.; Seth, B. D.; Guisinger, N. P., *Nanotechnology* **2015,** *26* (23), 235604.
24. Knorr, N.; Brune, H.; Epple, M.; Hirstein, A.; Schneider, M. A.; Kern, K., *Phys. Rev. B* **2002,** *65* (11), 115420.
25. Repp, J.; Moresco, F.; Meyer, G.; Rieder, K.-H.; Hyldgaard, P.; Persson, M., *Phys. Rev. Lett.* **2000,** *85* (14), 2981-2984.
26. Wahlström, E.; Ekvall, I.; Olin, H.; Walldén, L., *Appl. Phys. A* **1998,** *66* (1), 1107-1110.
27. Linderoth, T. R.; Horch, S.; Lægsgaard, E.; Stensgaard, I.; Besenbacher, F., *Phys. Rev. Lett.* **1997,** *78* (26), 4978-4981.

28. Wen, J. M.; Evans, J. W.; Bartelt, M. C.; Burnett, J. W.; Thiel, P. A., *Phys. Rev. Lett.* **1996,** *76* (4), 652-655.
29. Morgenstern, K.; Rosenfeld, G.; Lægsgaard, E.; Besenbacher, F.; Comsa, G., *Phys. Rev. Lett.* **1998,** *80* (3), 556-559.
30. Morgenstern, K.; Rosenfeld, G.; Comsa, G., *Phys. Rev. Lett.* **1996,** *76* (12), 2113-2116.
31. Schulze Icking-Konert, G.; Giesen, M.; Ibach, H., *Surf. Sci.* **1998,** *398* (1), 37-48.
32. Gross, D.; Grodsky, G., *J. Am. Chem. Soc.* **1955,** *77* (6), 1678-1680.
33. Barlow, S. M.; Raval, R., *Surf. Sci. Rep.* **2003,** *50* (6), 201-341.
34. Rankin, R. B.; Sholl, D. S., *J. Phys. Chem. B* **2005,** *109* (35), 16764-16773.
35. Rankin, R. B.; Sholl, D. S., *Surf. Sci.* **2005,** *574* (1), L1-L8.
36. Fischer, S.; Papageorgiou, A. C.; Marschall, M.; Reichert, J.; Diller, K.; Klappenberger, F.; Allegretti, F.; Nefedov, A.; Wöll, C.; Barth, J. V., *J. Phys. Chem. C* **2012,** *116* (38), 20356-20362.
37. Claridge, S. A.; Thomas, J. C.; Silverman, M. A.; Schwartz, J. J.; Yang, Y.; Wang, C.; Weiss, P. S., *J. Am. Chem. Soc.* **2013,** *135* (49), 18528-18535.
38. White, T. W.; Duncan, D. A.; Fortuna, S.; Wang, Y. L.; Moreton, B.; Lee, T. L.; Blowey, P.; Costantini, G.; Woodruff, D. P., *Surf. Sci.* **2018,** *668*, 134-143.
39. Marschall, M.; Reichert, J.; Weber-Bargioni, A.; Seufert, K.; Auwärter, W.; Klyatskaya, S.; Zoppellaro, G.; Ruben, M.; Barth, J. V., *Nat. Chem.* **2010,** *2*, 131.
40. Stepanow, S.; Lingenfelder, M.; Dmitriev, A.; Spillmann, H.; Delvigne, E.; Lin, N.; Deng, X.; Cai, C.; Barth, J. V.; Kern, K., *Nat. Mater.* **2004,** *3*, 229.
41. Grill, L.; Dyer, M.; Lafferentz, L.; Persson, M.; Peters, M. V.; Hecht, S., *Nat. Nanotechnol.* **2007,** *2*, 687.
42. Sykes, E. C. H.; Han, P.; Kandel, S. A.; Kelly, K. F.; McCarty, G. S.; Weiss, P. S., *Acc. Chem. Res.* **2003,** *36* (12), 945-953.
43. Kyriakou, G.; Boucher, M. B.; Jewell, A. D.; Lewis, E. A.; Lawton, T. J.; Baber, A. E.; Tierney, H. L.; Flytzani-Stephanopoulos, M.; Sykes, E. C. H., *Science* **2012,** *335* (6073), 1209-1212.
44. Kamna, M. M.; Graham, T. M.; Love, J. C.; Weiss, P. S., *Surf. Sci.* **1998,** *419* (1), 12-23.
45. Ling, W. L.; Bartelt, N. C.; Pohl, K.; de la Figuera, J.; Hwang, R. Q.; McCarty, K. F., *Phys. Rev. Lett.* **2004,** *93* (16), 166101.
46. Hannon, J. B.; Klünker, C.; Giesen, M.; Ibach, H.; Bartelt, N. C.; Hamilton, J. C., *Phys. Rev. Lett.* **1997,** *79* (13), 2506-2509.
47. Sholl, D. S.; Asthagiri, A.; Power, T. D., *J. Phys. Chem. B* **2001,** *105* (21), 4771-4782.
48. Clegg, M. L.; Driver, S. M.; Blanco-Rey, M.; King, D. A., *J. Phys. Chem. C* **2010,** *114* (9), 4114-4117.
49. Jones, G.; Gladys, M. J.; Ottal, J.; Jenkins, S. J.; Held, G., *Phys. Rev. B* **2009,** *79* (16), 165420.
50. Kresse, G.; Hafner, J., *Phys. Rev. B* **1993,** *48* (17), 13115-13118.
51. Kresse, G.; Hafner, J., *Phys. Rev. B* **1993,** *47* (1), 558-561.
52. Kresse, G.; Hafner, J., *Phys. Rev. B* **1994,** *49* (20), 14251-14269.
53. Kresse, G.; Furthmüller, J., *Phys. Rev. B* **1996,** *54* (16), 11169-11186.

54. Perdew, J. P.; Chevary, J. A.; Vosko, S. H.; Jackson, K. A.; Pederson, M. R.; Singh, D. J.; Fiolhais, C., *Phys. Rev. B* **1992,** *46* (11), 6671-6687.
55. Perdew, J. P.; Chevary, J. A.; Vosko, S. H.; Jackson, K. A.; Pederson, M. R.; Singh, D. J.; Fiolhais, C., *Phys. Rev. B* **1993,** *48* (7), 4978-4978.
56. Kresse, G.; Joubert, D., *Phys. Rev. B* **1999,** *59* (3), 1758-1775.
57. Methfessel, M.; Paxton, A. T., *Phys. Rev. B* **1989,** *40* (6), 3616-3621.

ACKNOWLEDGMENTS

Use of the Center for Nanoscale Materials, an Office of Science user facility, was supported by the U. S. Department of Energy, Office of Science, Office of Basic Energy Sciences, under Contract No. DE-AC02-06CH11357. EVI acknowledges support from the Chemistry and Biochemistry Department at the University of Tulsa. MCH acknowledges funding from the Office for Naval Research (N00014-14-1-0669).

COMPETING INTERESTS

The authors declare no conflict of interest.

CONTRIBUTIONS

EVI and NPG conceived the project; EVI and NPG carried out the experiment and data analysis. AJM and BK carried out the temperature diffusion experiment and analysis. RBR and SBD provided theoretical support and computational modeling. BLF provided engineering support for the experiment. EVI, NPG, RR, and MCH wrote and revised the manuscript. All authors contributed to the manuscript.

CORRESPONDENCE

nguisinger@anl.gov

Figure 1

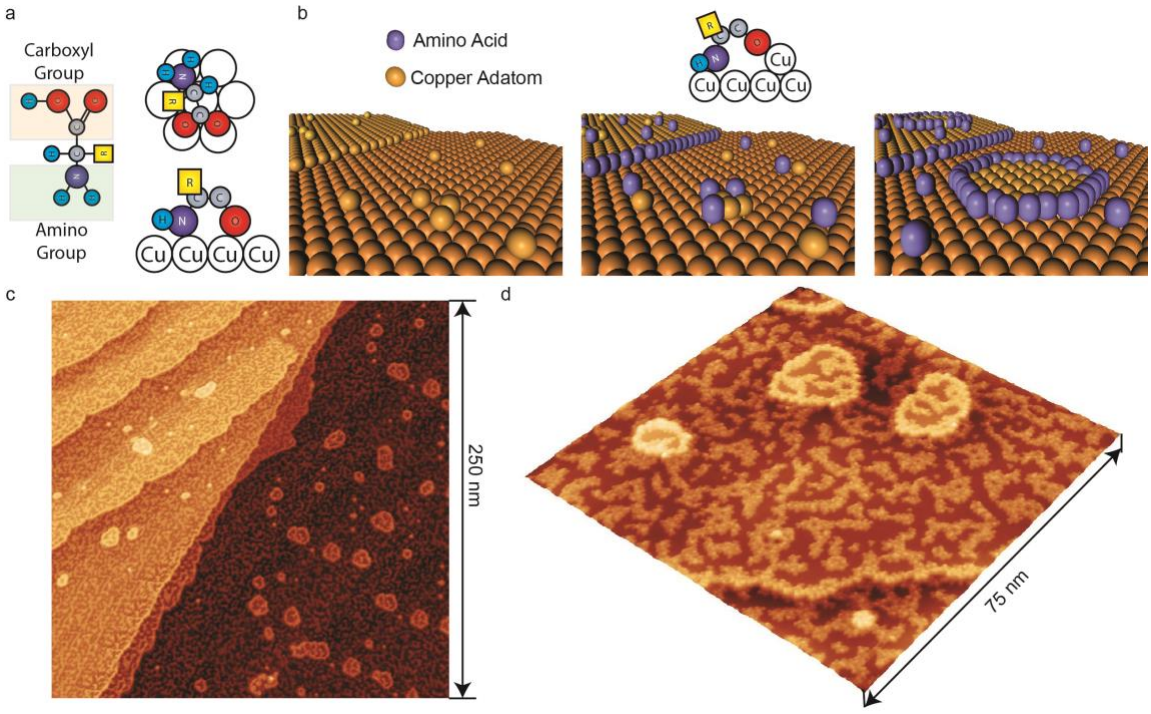

Figure 1: Two-dimensional separation between self-assembling amino acids and diffusing Cu atoms. a, Schematic model of an amino acid (left) identifying the carboxyl and amine groups. A schematic model of a deprotonated amino acid forming a planar tridentate bond with the surface. **b,** This schematic model represents the 2D separation process where the increase in amino acid coverage results in the formation of copper islands on the surface. The inset model shows a tridentate bond with a neighboring atom that results in immobilization of a diffusing copper atom. DFT calculations as described in Methods section indicate that the preferred binding motif is the tridentate footprint as shown, with the carboxylate tail on the step edge of the adisland. This configuration is lower in energy by 0.18 eV/molecule compared to a tridentate footprint with the amine group on the step edge, and 0.32 eV compared to a bidentate footprint with one oxygen from the carboxylate group on the step edge. The aforementioned energies were for a single adsorbate per ad-island. When the adsorbing isoleucine coverage was increased to a full monolayer (6 per 19 atom island), the average adsorption energy per molecule decreased by 0.05 eV/molecule. **c**, STM image of copper islands imbedded in a self-assembled matrix of isoleucine molecules (coverage < 1 ML). **d**, This zoomed in STM image shows the tight ordering of the amino acids surrounding the copper islands and step-edges.

Figure 2

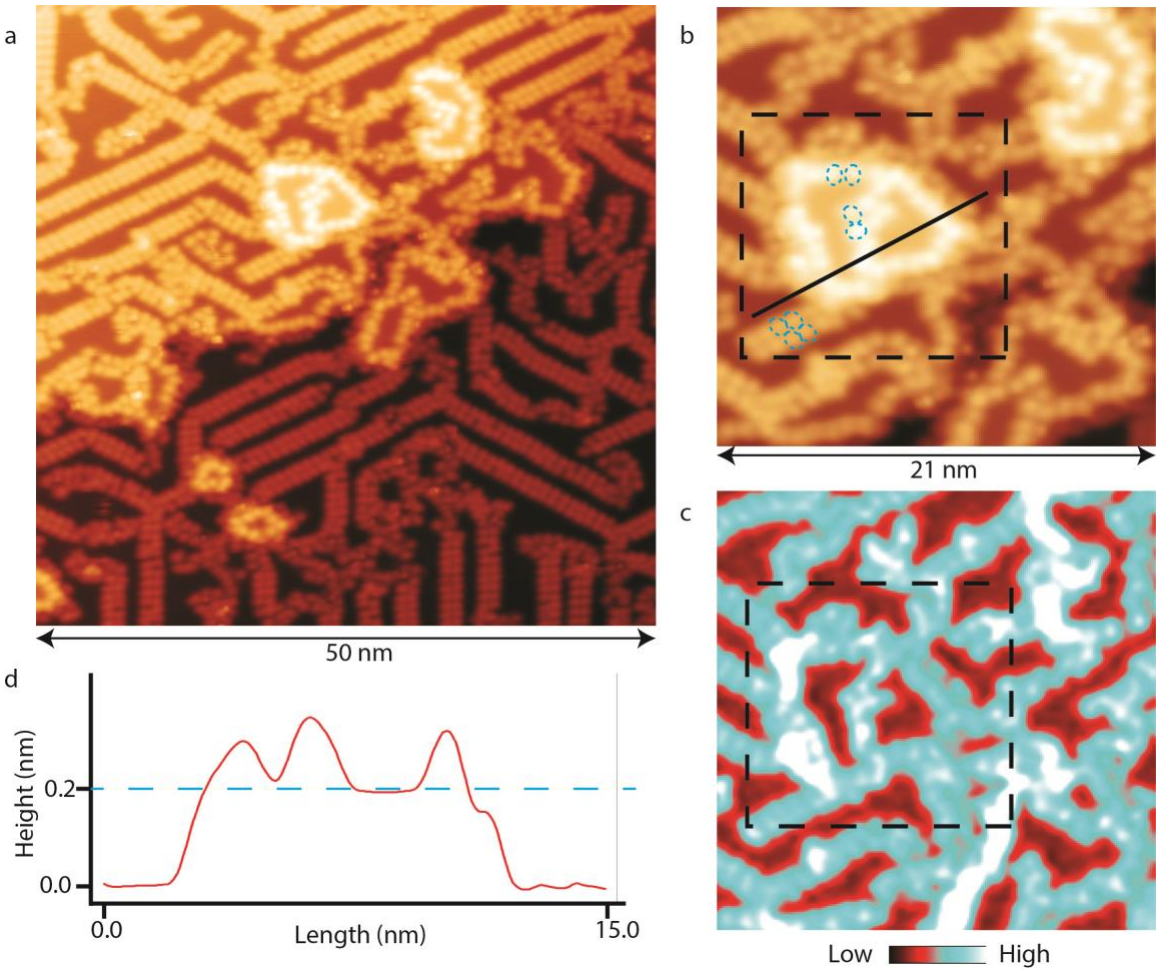

Figure 2: Verification of metallic islands. a, STM topographic image showing copper islands imbedded in the network of self-assembled tryptophan chains. **b**, Zoomed in STM image of an imbedded island which contains areas of bare Cu. Notice that molecular self-assembly has also started on top of this small island. The STM can resolve the individual amino acids as outlined by dashed circles. **c**, 2D conductance dI/dV mapping shows that the bare copper on the island has the same LDOS as the surrounding bare copper on the terrace, where the rectangular area is the same in **b** and **c**. **d**, Line profile of the island (solid line in **b**) indicates that the bare regions of the island are consistent with the step-height of Cu(111) ~ 0.2 nm.

Figure 3

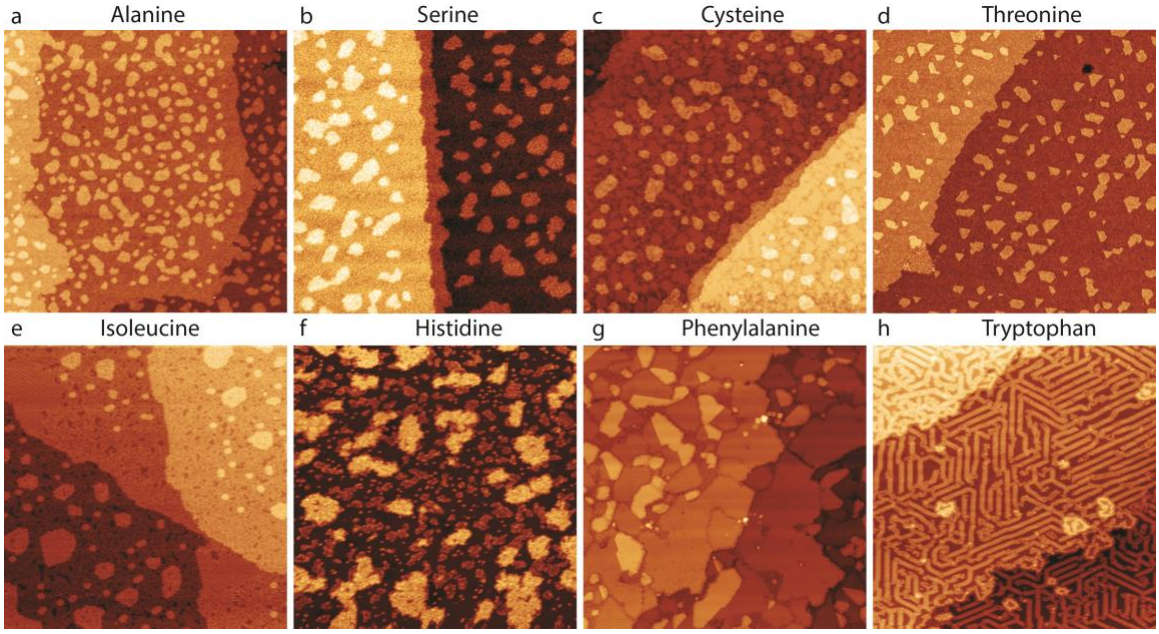

Figure 3: Cu immobilization appears to be universal for a range of amino acid structures. This series of STM images (200 nm x 200 nm) show Cu islands forming within different self-assembled amino acid networks. The immobilization is most pronounced when there is close to a full monolayer of amino acids on the surface. Additionally, the higher the dose, the faster the surface is covered with amino acids, which also affects the separation. The following amino acids are shown: **a**, alanine; **b**, serine; **c**, cysteine; **d**, threonine; **e**, isoluceine; **f**, histidine; **g**, phenylalanine; and **h**, tryptophan, which represent a good cross-section of various amino acid functionality.

Figure 4

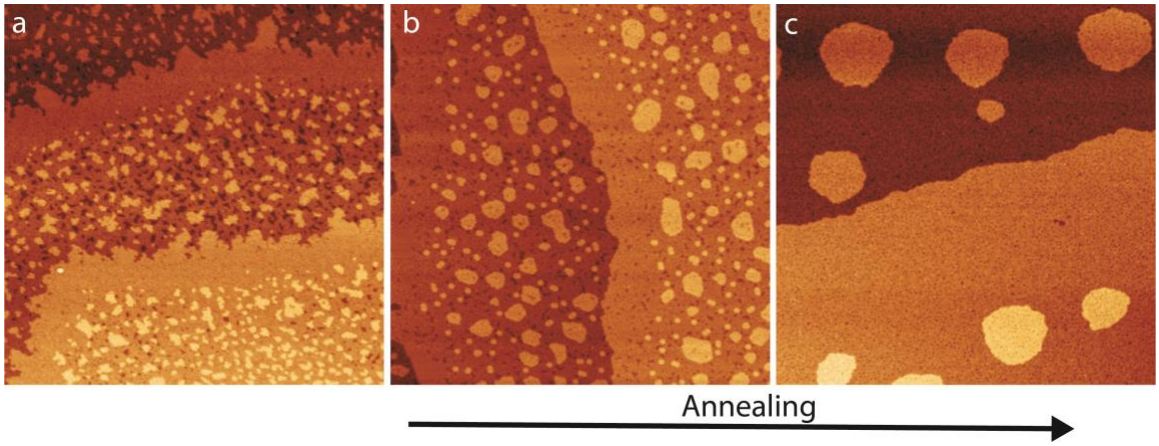

Figure 4: Temperature evolution of immobilized Cu atoms within an isoleucine network. Althought the Cu adatoms are immobilized withing the amino acid molecular network, they are capable of diffusion when given sufficient thermal energy. All STM images are 250 nm x 250 nm. **a**, This STM image shows a surface after deposition at room temperature with no thermal annealing. Rather than islands there are small clusters imbedded in the molecular networks **b**, Following our standard 15 min. anneal at 450 K, the small Cu clusters diffuse to form larger islands. **c**, After annealing for 90 min. the Cu adatoms coalesce to form large islands. It is at this point that we begin to observe a breakdown in Ostwald ripening.

Figure 5

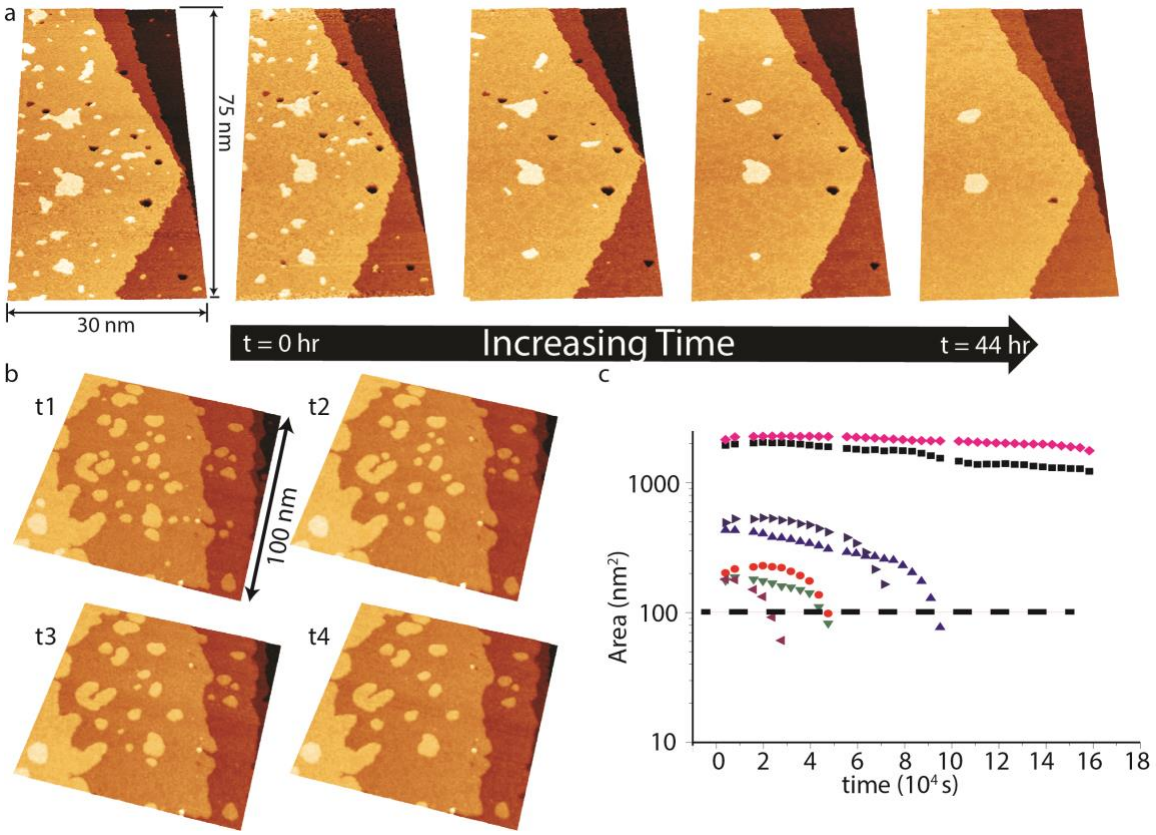

Figure 5: The immobilization disrupts Ostwald ripening. The amino acid immobilization of Cu atoms presents an interesting system for studying surface diffusion and metal transport. Cu islands on a clean surface will follow Ostwald ripening, where larger islands grow and smaller islands decay with time, and should be observable at room temperature. The presence of the amino acids disrupts this process. **a,** At an elevated temperature (350 K), a full monolayer of cysteine molecules and Cu islands were imaged over the same area for a period of 44 hrs. The STM images show that several islands shrink and disappear with time. At the end of this time sequence, only a couple of the larger islands remain and are smaller in size. **b**, A similar decay pattern is observed for a monolayer of isoleucine. Although it is a shorter time period between t1 and t4 relative to the cysteine system, several of the smaller islands decay, while the larger remaining islands shrink in size. **c**, In the statistical analysis of the cysteine islands which plots the island area vs. time, a trend in the decay patterns can be observed. The smaller islands decay much faster than the larger islands and at a critical area (dashed line) the islands disappear.

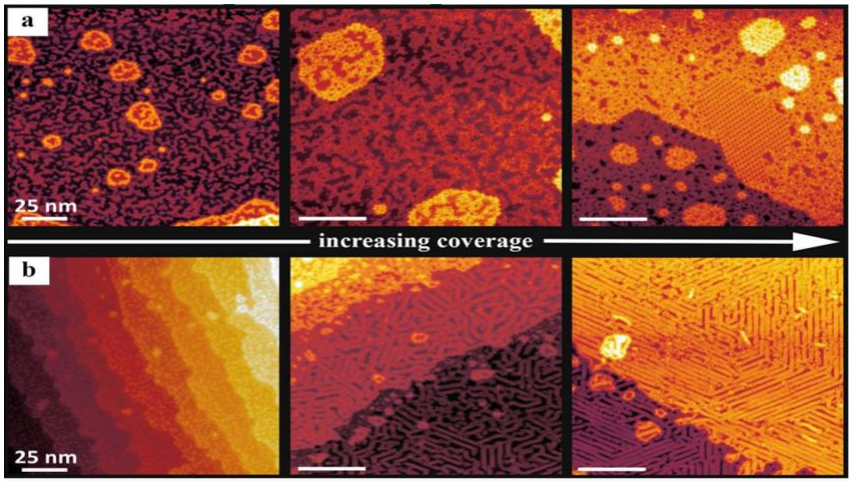

Figure Supplemental #1. Effect of molecular surface coverage on formation of Cu islands. a, Increasing coverage of Isoleucine indicated that as more molecules are added to the surface, the Cu islands grow in both number and size. In addition, the presence of magic clusters increased with molecular coverage. As more molecules were added to the surface, the diffusion of surface metal atoms was increasingly more suppressed and the molecules assisted in the capture of more atoms into islands and clusters. **b,** Increasing coverage of Tryptophan showed a similar growth in the size of the islands and the perturbation of the step edges.